Online ISSN: 2981-0396 Print ISSN: 2981-0388

International Journal of Iron & Steel Society of Iran

Journal Homepage: https://journal.issiran.com/

Research Article

Using Recycled Machining Chips and Reduced Graphene Oxide in Spot Welding of Galvanized Sheets to Improve Hardness and Corrosion Resistance

S. M. R. Sedehi *[1], S. H. Yazdi [2], F. Norouzi Palangani [3], Z. Maleki [4], R. Poudinehei [5]

[1] *Department of Mechanical Engineering, College of Engineering, University of Tehran, Tehran, Iran*
[2] *Aseman Nano Part Company, Gonabad, Iran*
[3, 4] *Nano Part Aseman Co, Gonabad, Iran*
[5] *Department of Mechanical Engineering, Ferdowsi University of Mashhad, Mashhad, Iran*

ARTICLE INFO

Keywords:

Spot Welding, Galvanized Sheet, RGO, Recycling, Chip, CK45.

Article history:

Received 23 April 2024
Received in revised form 05 August 2024
Accepted 26 November 2024

ABSTRACT

In recent years, spot welding has received increasing attention from metal sheet-related industries due to its efficiency, high speed, and low operational costs. This study aims to enhance the spot welding properties of galvanized sheets by incorporating carbon-based and metallic reinforcements, utilizing recycled steel powder and synthesized reduced graphene oxide (RGO). The welding zone characteristics were analyzed using Scanning Electron Microscopy (SEM), X-ray Diffraction (XRD), hardness, and corrosion tests. The results from the conducted tests confirm the beneficial effects of incorporating RGO and recycled steel powder. The findings from the hardness and corrosion tests further validate the positive influence of RGO and recycled steel shavings powder on the material's performance. The hardness and corrosion resistance values improved significantly, with the unreinforced sample showing 209 HV and 0.25 µm/year, compared to 261.8 HV and 0.1 µm/year for the optimally reinforced sample.

1. Introduction

Galvanized steel sheets are extensively utilized across various industries owing to their lightweight nature, environmental friendliness, high strength, and excellent corrosion resistance [1]. Temporary connections, which require the disassembly and reassembly of components, commonly employ mechanical fasteners. Such connections necessitate the drilling of holes, which are susceptible to stress concentration, potentially resulting in a reduction in structural strength. Moreover, the use of screws and rivets adds weight to the structure, compromising design objectives focused on lightweight construction [2–5]. Permanent connections are typically achieved through adhesive bonding or welding techniques. Adhesive bonding demands meticulous surface preparation, and its performance is highly influenced by factors such as environmental conditions, temperature, curing time, and the specific adhesive type used. No single adhesive formulation can meet the requirements of all applications [6–9]. Adhesive bonds provide superior stiffness, enhanced shear strength, and more uniform load distribution compared to mechanical fasteners or welding [10–12]. Welding, a widely used method for permanent connections, is categorized into fusion welding and solid-state welding. Fusion welding involves melting the surfaces of base metals until they reach their

* *Corresponding Author*
Email: mrsedehi@ut.ac.ir
Address: Department of Mechanical Engineering, College of Engineering, University of Tehran, Tehran, Iran
1.Ph.D. Candidate, 2. B.S, 3. B.S, 4. B.S, 5.Ph.D. Candidate

DOI: http://10.22034/IJISSI.2024.2027196.1289
Published by ISSI (Iron & Steel Society of Iran)

melting point, facilitating their union during the welding process. Common techniques include resistance spot welding (RSW), arc welding (AW), and resistance seam welding (RSSEW). In contrast, solid-state welding bonds the surfaces of base metals without heating them to their melting point, with examples including friction welding (FW) and ultrasonic spot welding (USW). Although mechanical fasteners and adhesive bonds are suitable for joining dissimilar materials and composites, welding, despite its inherent limitations, is often preferred for its compatibility with process automation and high production speed. Spot welding is particularly prevalent in the automotive industry, where a car body typically incorporates thousands of spot welds [13, 14]. On the other hand, resistance spot welding (RSW) is an efficient method for joining metal sheets, widely recognized across industries for its speed, cost-effectiveness, and compatibility with automation. The reliability and mechanical performance of spot welds are critical in ensuring safety and structural integrity during vehicle collisions [15]. Graphene, with its significant electrical and thermal conductivity [16], high Young's modulus [17], and desirable tensile strength [18], has shown special appeal as a reinforcement for enhancing spot welding properties. Introduced in 2010, graphene, a two-dimensional nanomaterial, has been utilized for its unique tensile strength, up to 200 times that of steel, and its ability to react to form hard phases, along with desirable wear resistance, in various applications [19]. Industrial activities in 2021 directly contributed to the emission of 4.9 gigatons of CO_2, representing one-fourth of global emissions. Among these, iron and steel production accounted for 30% of the world's CO_2 emissions in 2021. This trend is on the rise as industrial emissions have increased by over 70% from 2000 to the present, driven by a slight increase in energy efficiency alongside a growing global demand for industrial goods [20]. Predictably, separating material demand from economic and population growth can contribute to reducing CO_2 emissions. One primary pathway for reducing primary material production and resource separation from economic growth involves implementing circular economy strategies, including longer product lifecycles, repair, product upgrades, modularity, remanufacturing, component reuse, and recycling. Solid-state recycling strategies, particularly using machining waste powders, have been tested and improved [21]. In summary, metal machining chips, traditionally regarded as waste, are often sent for melting, thereby erasing their processing history entirely. Alternatively, these metal chips can be effectively utilized as raw materials for spot welding reinforcement, providing a sustainable solution compared to conventional thermomechanical recycling routes. Akbari et al. [22] presented an algorithm for optimizing resistance spot welding and enhancing joint strength, showing a significant increase in fracture force by selecting the correct positions for two, three, and four spot welds. In another study, Morad et al. [23] investigated the effect of welding point diameter on the strength of galvanized sheet connections. The results showed that the diameter of the spot weld does not affect the microhardness of the weld zone, but as the spot diameter increases, the weld strength also increases. Khosravi et al. [24] in an interesting study examined the effect of graphene oxide and revived graphene oxide nano-sheets at different concentrations on arc spot welds. The results of these studies showed that with an increase in RGO concentration up to 10 mg/ml, the tensile strength and hardness of the weld metal improved by 5.20% and 38.4%, respectively. Dong et al. [25] used graphene nanoplates to improve the strength of aluminum alloy connections in spot welding. They found that fatigue life and tensile strength of the connections significantly increased with the addition of this reinforcement. In another research, Das et al. [15] investigated the effect of graphene nanoplate on improving the mechanical properties of galvanized steel in spot welding. The results indicated a 124% increase in strength, ductility, and a reduction in the brittleness of the spot weld. Eisi et al. [26] reported on the effect of graphene on the strength and microhardness of copper-aluminum connections in friction stir welding. These studies showed that adding graphene to the copper-aluminum connection significantly increased the shear strength and microhardness of the joint while reducing the resistivity of the alloy. The improved mechanical properties of graphene-reinforced connections make them ideal for a wide range of applications, highlighting the critical role of recycling and reusing metal machining waste to promote sustainability in industrial practices. To address the need for enhanced strength in spot welding, reduced graphene oxide (RGO) and recycled machining chips are introduced as innovative reinforcements. RGO, with its exceptional mechanical, thermal, and electrical properties, significantly improves the strength, heat transfer efficiency, and fatigue resistance of welds. At the same time, utilizing recycled machining chips not only minimizes costs and industrial waste but, when combined with RGO, further enhances the mechanical performance of welds. These innovations create significant advancements in industries such as automotive, aerospace, and electronics, which require strong and lightweight connections, demonstrating that the combination of nanotechnology and material recycling can lead to significant progress in industrial processes.

2. Materials and Experiments

2.1. Production of Raw Materials for the Experiment: Machining Chips and Reduced Graphene Oxide (RGO)

Steel chips were produced from CK45 steel shafts through a closed machining cycle with parameters specified in Table 1. and Fig. 1. This machining process took

place in an industrial production center, and the cutting parameters listed in Table 1. reflect common industrial machining practices, ensuring that the characteristics of the chips used are representative of those produced in the manufacturing industry. Graphene oxide was prepared from graphite powder using a modified Hummers' method [27]. A 200 mL aqueous solution of graphene oxide with a concentration of 2.5 mg/mL was prepared and subjected to ultrasonic waves for 1 hour to achieve dispersion. When working with the ultrasonic device, to prevent the suspension and tipping of laboratory beakers containing solution materials, these containers should be manually adjusted before starting the process. For reduction, the suspension was placed inside an autoclave under hydrothermal conditions for 12 h at a temperature of 190 °C and a pressure of 12 bars. The resulting hydrogel product then underwent freeze-drying at -50 °C for 12 h to remove absorbed water and form a porous network structure [28].

2.2. Powder Composition and Characterization

As shown in Fig. 1. to achieve a homogeneous final gel composition, RGO powder was dispersed using an ultrasonic device for 45 min. To more precisely investigate the reinforcing behavior of the weld joint with recycled steel powder, this material was also converted to powder using a ball mill and added to the mixture along with RGO. The composition ratios are provided in Table 2. Before starting the resistance spot welding process, the surfaces of galvanized sheets were cleaned with silicon carbide paper with a mesh size of 2000-400, dried, and prepared with a clean stone. The fixation of the two sheets was done using a perforated template, and the reinforcing agent mixture was injected at a specified point on the sheets. The welding of the two sheets was carried

Table 1. Material Properties Under Investigation.

Galvanized sheet

Element	Fe	Al	S	p	Mn	Si	C
Composition (%w)	Balance	0.051	0.008	0.012	0.207	0.009	0.033

CK45

Element	Fe	Si	Cr	C	P	Mn	S
Composition (%w)	Balance	0.25	0.27	0.46	0.1	0.57	0.1

RGO

E	P	Elongation	Ther conductivity	Electrical conductivity
1060 GPA	1 g/cm^2	20%	3000W/MK	15000 cm^3/v.s

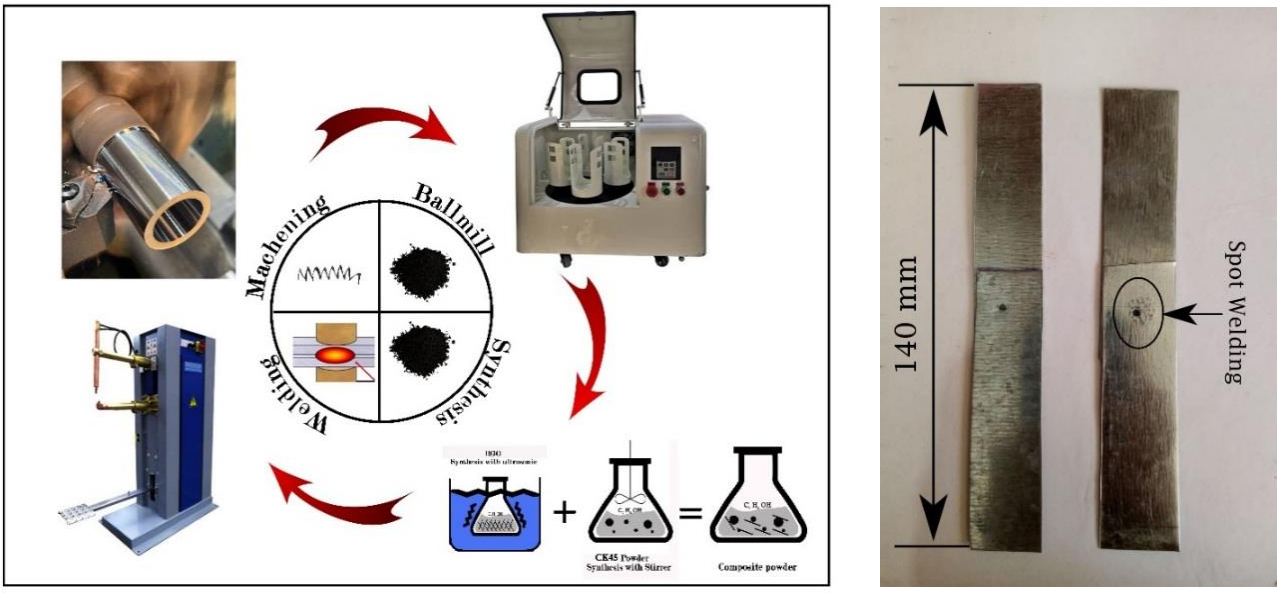

Fig. 1. Schematic of the Process Steps and Dimensions of the Sheet.

out using a welding machine model 4645N-16KVA with optimal parameters as listed in Table 3. After producing the samples, X-ray diffraction (XRD) was performed on the samples to examine the phases present, using an Explorer device from GNR Italy under the conditions of V=40Kv and Current=30mA. Morphological changes in the welded samples were also investigated using a Scanning Electron Microscope (SEM) model MIRA3 from TESCAN, Czech Republic, with a resolution capability of up to 1.5 nm at a voltage of 15 Kv. The hardness of the samples was measured using the Vickers method with an INNOVATEST NEXUS 8000XL hardness tester, applying a 612.9 N tungsten carbide indenter with a diameter of 2.5 mm and a holding time of 15 sec, according to ASTM A370 (2020) standard. To obtain an average value, the hardness test was repeated at least three times for each sample. Electrochemical corrosion tests on the samples were conducted in the voltage range of -250 to +250 mV, with a scan rate of 1 mV and an OCP duration of 1200 sec.

3. Discussion and Conclusion

3.1. XRD

XRD analysis was conducted to identify the phases formed in the weld area, and the results are shown on the produced samples in Fig. 2. As indicated in the figure, during the chip extraction and production stages of recycled CK45, the steel powder contains phases with peaks at 110, 200, and 211, corresponding to iron phases. The 110 peak corresponds to the austenite phase (γ-Fe), the 200 peak corresponds to the ferrite phase (α-Fe), and the 211 peak can correspond to either the martensite phase (α'-Fe) or the ferrite phase (α-Fe). Furthermore, the peaks observed at 73 and 78 degrees correspond respectively to the phases of iron (Fe) and iron carbide (Fe_3C). The no significant change in the nature and integrity of the metal has occurred, indicating the success of this stage. The presence of a 26.5-degree peak in the chart also indicates the presence of RGO in the samples, demonstrating proper control over the production conditions. Additionally, weaker peaks corresponding to the iron phases, mainly attributed to the presence of steel chips, are observable.

3.2. Morphological Examination by SEM

SEM images of various points on the produced samples are shown in Fig. 3. where the bond interface and the injection lines of the reinforcements into the melted structure are clearly visible. Image (a) illustrates the microstructure of the base metal, revealing a dark-colored ferritic structure, a light-colored martensitic structure, and the remaining regions being austenitic. As observed, the ferrite content in the base metal is higher than that of martensite. In the Heat-Affected Zone (HAZ), the temperature is lower than in the Fusion Zone (FZ), so a complete transformation from austenite to martensite does not occur. It is evident that the ferrite and martensite levels are nearly equal in Image (b), representing the HAZ region. In Image (c), which depicts the boundary between the weld and the HAZ, a reduction in ferrite content is observed. Finally, in Image (d), due to complete melting and rapid thermal cycles during spot welding, a martensitic structure is formed.

Table 2. Sample Naming.

Sample	Type of Reinforcement
R1	-
R2	100%W RGO
R3	50W% RGO +50W% Chip (0/5 mm)
R4	50W% RGO +50W% Chip (1 mm)
R5	50W% RGO +50W% Chip + Balmil (0/5 mm)
R6	50W% RGO + 50W% Chip (1/5 mm)

Table 3. Welding Process Parameters.

Welding process variables			
Tungsten rod diameter, (mm)	Welding current, (kA)	Welding time, (cycle)	Electrode force, (kN)
4	10-26	10	2/1
Machining process variables			
Cutting speed, (rpm)	cutting depth, (mm)	Feed rate, (mm)	Coolant
350	0/5	0/1	-

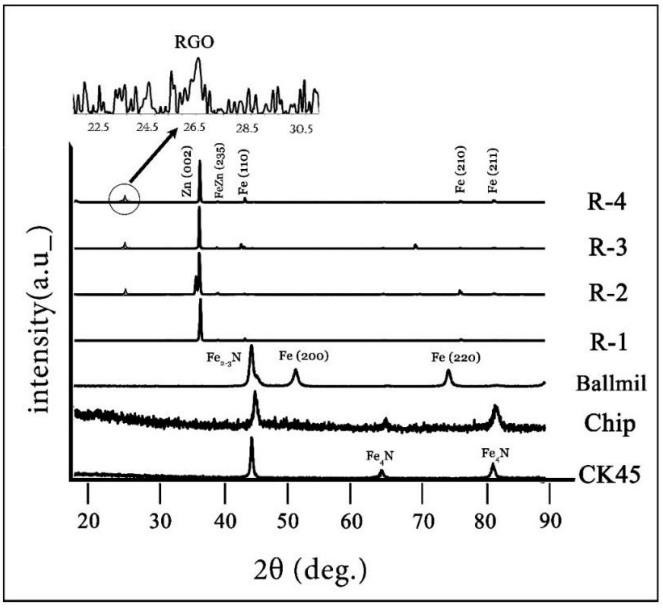

Fig. 2. XRD Results of Different Stages in the Process.

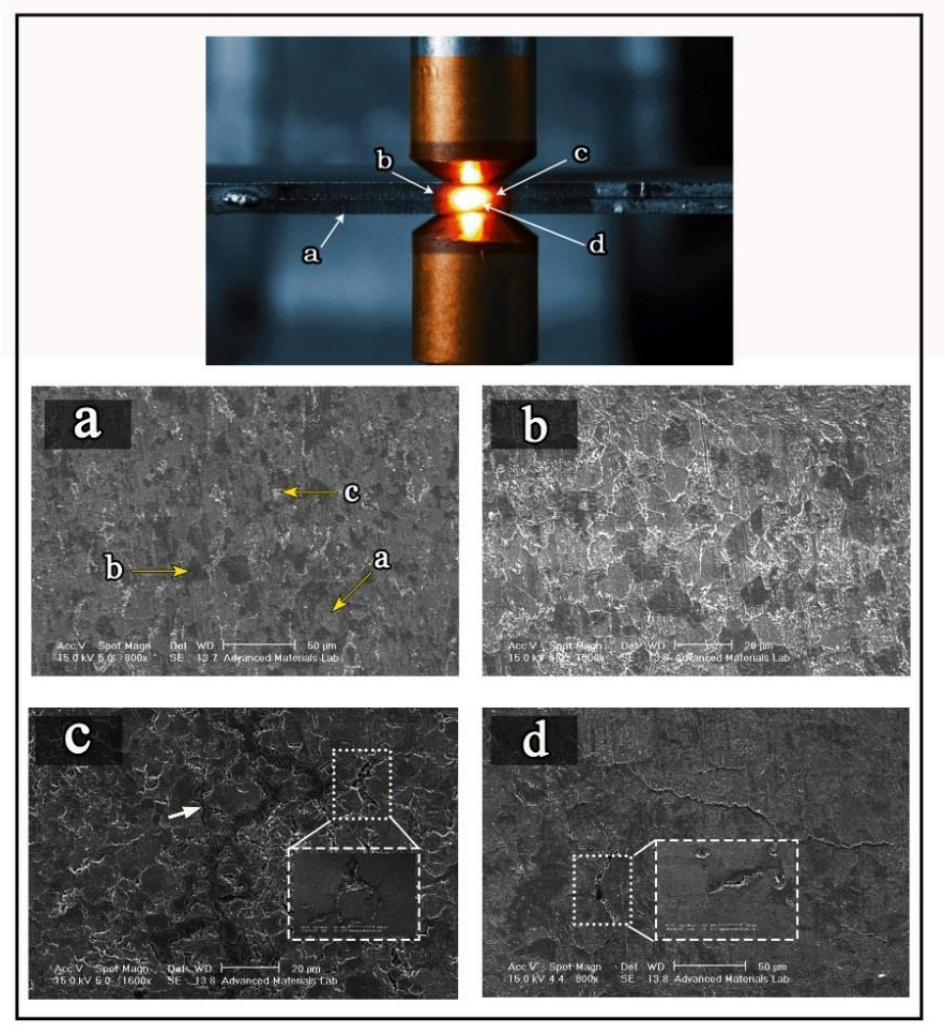

Fig. 3. SEM Images a) Base metal body, b) Heat-Affected Zone (HAZ), c) Boundary between FZ and HAZ, and d) Fusion Zone (FZ).

3.3. Hardness

Changes in microhardness characteristics in the presence of various types of reinforcements are illustrated in Fig. 4. After examining the Vickers microhardness test results from the weld zone, sample R5 exhibited the best outcome. Weld hardness is directly influenced by the phases formed during the welding process and the presence of reinforcements. Hardness test results from the weld zone indicated that sample R5, with its reinforcement compositions, has the highest average hardness, showing a significant increase compared to the untreated sample. Given the constant weight percentage of RGO, the fluctuations in hardness values are attributed to the type of recycled steel powder. The addition of 50% by weight RGO resulted in a slight reduction in hardness. The highest recorded value is also in sample R5, which utilized both RGO and ball-milled recycled steel chips as reinforcements. Therefore, the optimal thickness of the chips and the uniform distribution of ball-milled powder relative to recycled chips play a significant role in the hardness and its variations. By consolidating the obtained results, it can be concluded that adding RGO and recycled steel powder up to an optimal level increases hardness, and beyond that, it leads to a decrease in the hardness of the weld zone. The presence of inclusions and recycled metal chips from steel machining can alter the chemical composition, microstructural arrangement, and residual stress distribution in spot weld regions. The presence of these materials may lead to the formation of hard phases, mechanical discontinuities, changes in cooling rate and heat transfer, and the generation of local stresses-factors that could potentially increase the localized hardness of the weld zone. Understanding the impact of these factors can be further refined through future experimental tests and supplementary microscopic studies in the field of mechanics. Higher hardness in spot welds enhances wear and corrosion resistance, which is particularly important in industries such as automotive, aerospace, and heavy equipment manufacturing. Spot welds with optimal hardness can withstand heavier loads and are commonly used in engineering structures, such as car bodies, metal frameworks, and mechanical components. This attribute contributes to a longer service life and reduced maintenance requirements, which is crucial in industries like automotive manufacturing and the mass production of metal parts, where access to weld points is often difficult. In industries where safety is paramount, such as rail transportation and aerospace, suitable hardness in spot welds can prevent sudden failures and ensure safety. Additionally, appropriate hardness serves as a quality control indicator in production processes, helping to ensure uniformity and structural integrity of manufactured parts. Overall, the hardness level of spot welds has a direct impact on the performance, safety, and lifespan of industrial components and structures, making it highly significant in many industrial applications.

3.4. Potentiodynamic Polarization Corrosion

To measure corrosion, Tafel slopes were plotted in the linear region of polarization curves, and polarization resistance was calculated based on the Stern-Geary equation provided below [29] :

$$R_P = \frac{b_a b_c}{2.303(b_a+b_c)i_{corr}} \quad \text{Eq.(1)}$$

$$i_{corr} = \frac{B}{R_P} \quad \text{Eq.(2)}$$

$$B = \frac{b_a b_c}{2.303(b_a+b_c)} \quad \text{Eq.(3)}$$

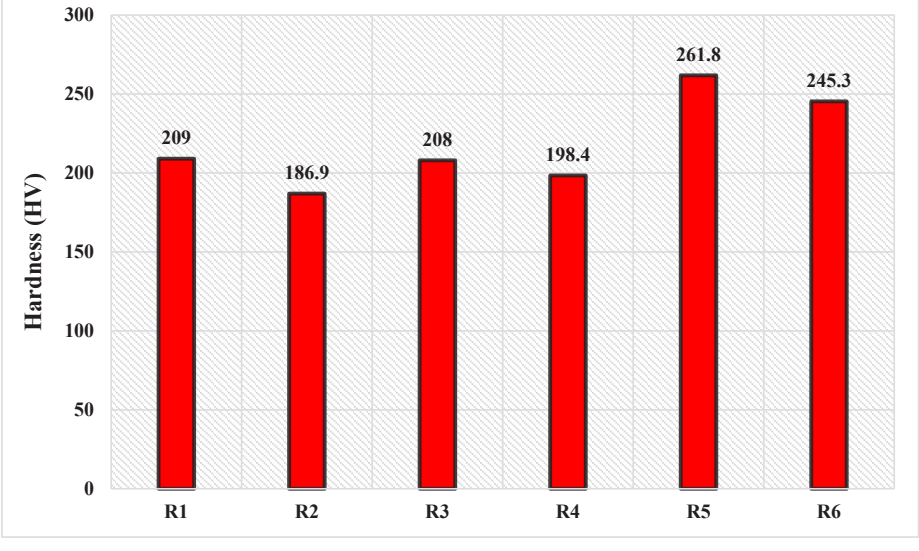

Fig. 4. Vickers Microhardness Results.

In the equation, R_p represents the Linear Polarization Resistance (LPR) of the produced sample, b_a and b_c are the anodic and cathodic Tafel slopes, respectively. I_{corr} is the corrosion current density, and E_{corr} is the corrosion potential. Fig. 5. shows the potentiodynamic polarization test of the sample without the reinforcement compared to the samples with reinforcements. According to the data extracted from the Stern-Geary equation [19], the corrosion potential has changed from -1.0234 for the sample without reinforcement to -1.008 for sample R4, indicating a decrease in thermodynamic corrosion likelihood in these samples [30]. Additionally, the corrosion current density of sample R1 has decreased from 6.5066 µA per square centimeter to 0.00014648 µA per square centimeter in sample R5. Due to the injection of RGO and ball-milled steel reinforcement into the samples, the corrosion current is reduced by more than 6 times compared to the sample without reinforcement. Past research suggests that if the corrosion potential increases and the corrosion current density decreases, the corrosion of the sample decreases [31], which is confirmed in the produced samples of this study. Finally, the corrosion rate in micrometers per year for the produced samples indicates that the sample with RGO shows a slight decrease in the corrosion rate compared to the sample without reinforcement. While the ball-milling process positively impacts mechanical properties, it exhibited the worst performance in terms of corrosion rate. In contrast, RGO significantly reduces the corrosion rate in spot welds through multiple mechanisms. It enhances uniform load distribution, acts as a physical barrier against corrosive agents, and possesses inherent anti-corrosive properties. Additionally, RGO increases the electrical resistance of the weld area, effectively lowering the corrosion current. Additionally, it improves the mechanical properties, such as hardness and strength, which minimizes micro-cracks and corrosion-induced fractures. RGO also reduces the concentration of active corrosive ions by adsorbing them. Scientific studies confirm that incorporating RGO into metals substantially enhances their corrosion resistance by providing physical and electrochemical protection, improving mechanical characteristics, and limiting the penetration of corrosive substances.

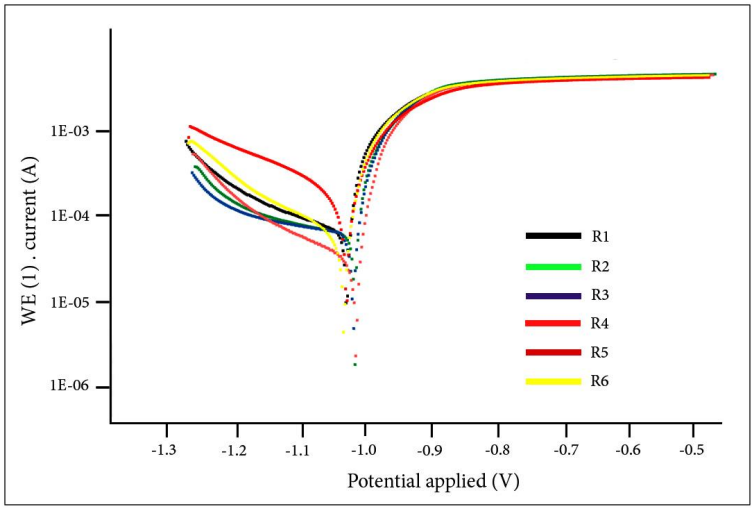

Fig. 5. The potentiodynamic polarization test curves.

Table 4. Corrosion Test Results.

Parameter	R1	R2	R3	R4	R5	R6
E_{corr} (V)	-1/0234	-1/01	-1/0127	-1/008	-1/237	-1/0277
i_{corr} (µA/cm^2)	6/5066 E_0.5	5/653 E_0.5	5/7811 E_0.5	2/6204 E_0.5	0/00014648 E_0.5	5/1804 E_0.5
b_a (V/dec)	0/034786	0/031357	0/039804	0/031875	0/074495	0/037711
b_c (V/dec)	0/44567	0/68609	0/77318	0/2632	0/19124	0/23207
R_p (ohm)	215/37	230/37	284/34	470/98	158/95	271/95
Corrosion rate (µm/year)	0/25708	0/22335	0/22841	0/10353	0/57875	0/20468

5. Conclusions

In this study, the effects of RGO and recycled CK45 steel powder on the spot welding efficiency of galvanized sheet metal were systematically investigated. The study yielded several noteworthy findings regarding the changes in the mechanical properties of the weld zone:

- Ball-milled recycled steel powder, compared to the original recycled steel, has a better effect on the tensile strength and hardness of the weld zone, likely due to a more uniform distribution and better dissolution in the weld zone.
- The thickness of the chip has optimally increased hardness of the welded joint, followed by a decreasing trend.
- Samples containing RGO showed a slight reduction in the corrosion rate compared to samples without a reinforcing agent, and the ball-milling process, contrary to its positive effect on mechanical properties, yielded the worst result in terms of corrosion rate.

These findings point to the complexity of the interactions among various parameters in the welding process, where the selection of reinforcing agents, their distribution, and the powder thickness play critical roles in determining the mechanical and corrosion properties of the welded joints. Future research could focus on variations in thickness and machining conditions for the production of recycled powder.

Appreciation and Thanks

The authors of this article deem it necessary to express their sincere gratitude to Ms. Mohddeseh Moradgholi (Iran - Zahedan) for her extensive support in facilitating this research.

References

[1] Puleo R, Latif A, Ingarao G, Di Lorenzo R, Fratini L, Solid bonding criteria design for aluminum chips recycling through Friction Stir Consolidation, J Mater Process Technol. 2023; 319: 118080.

[2] Lionetto F, Balle F, Maffezzoli A, Hybrid ultrasonic spot welding of aluminum to carbon fiber reinforced epoxy composites, J Mater Process Technol. 2017; 247: 289–295.

[3] Cheng X, Wang S, Zhang J, Huang W, Cheng Y, Zhang J, Effect of damage on failure mode of multi-bolt composite joints using failure envelope method, Compos Struct. 2017; 160: 8–15.

[4] Choi J.I, Hasheminia S.M, Chun H.J, Park J.C, Chang H.S, Failure load prediction of composite bolted joint with clamping force, Compos Struct. 2018; 189: 247–255.

[5] Huang Y, Meng X, Xie Y, Wan L, Lv Z, Cao J, et al. Friction stir welding/processing of polymers and polymer matrix composites, Compos Part A Appl Sci Manuf. 2018; 105: 235–257.

[6] Goushegir S, dos Santos J, Amancio Filho S, Friction Spot Joining of aluminum AA2024/carbon fiber reinforced poly(phenylene sulfide) composite single lap joints: Microstructure and mechanical performance, Mater Des. 2014; 54: 196–206.

[7] Jeevi G, Nayak S.K, Kader M.A, Review on adhesive joints and their application in hybrid composite structures, J Adhes Sci Technol. 2019; 33: 1497–1520.

[8] Maggiore S, Banea M.D, Stagnaro P, Luciano G, A Review of Structural Adhesive Joints in Hybrid Joining Processes, Polymers. 2021; 13: 3961.

[9] Lambiase F, Scipioni S.I, Lee C.J, Ko D.C, Liu F, A State of the Art Review on Advanced Joining Processes for Metal Composite and Metal Polymer Hybrid Structures, Materials. 2021; 14: 1890.

[10] Antelo J, Akhavan Safar A, Carbas R, Marques E, Goyal R, da Silva L, Replacing welding with adhesive bonding: An industrial case study, Int J Adhes Adhes. 2021; 113: 103064.

[11] Offerman B, Abke T, Barker M, Vivek A, Daehn G.S, Mechanical properties of joints in 5052 aluminum made with adhesive bonding and mechanical fasteners, Int J Adhes Adhes. 2018; 83: 96–102.

[12] Braga D.F, Maciel R, Bergmann L, da Silva L.F, Infante V, dos Santos J.F, et al. Fatigue performance of hybrid overlap friction stir welding and adhesive bonding of an Al-Mg Cu alloy, Fatigue Fract Eng Mater Struct. 2018; 42: 1262–1270.

[13] Paulraj C, Raj V.J, An intelligent model for defect prediction in spot welding, Turk J Comput Math Educ. 2021; 12: 3991–4002.

[14] Pouranvari M, Marashi S.P.H, Critical review of automotive steel spot welding: Process, structure and properties, Sci Technol Weld Join. 2013; 18: 361–403.

[15] Beck S.C, Williamson C.J, Kinser R.P, Rutherford B.A, Williams M.B, Phillips B.J, et al. Examination of microstructure and mechanical properties of direct additive recycling for Al-Mg-Mn alloy Machine chip waste, Mater Des. 2023; 228: 111733.

[16] Xie Z, Zhang A, Yan W, Zhang Y, Mu T, Yu C, Study on shear performance and calculation method for self-pierce riveted joints in galvanized steel sheet, Thin-Walled Struct. 2021; 161: 107490.

[17] Das T, Panda S.K, Arora K.S, Paul J, Investigation of the microstructure and mechanical behavior of resistance spot-welded CR210 steel joints using graphene as an interlayer, Mater Chem Phys. 2023; 302: 127693.

[18] Balandin A.A, Ghosh S, Bao W, Calizo I, Teweldebrhan D, Miao F, et al. Superior thermal conductivity of single-layer graphene, Nano Lett. 2008; 8(3): 902–907.

[19] Novoselov K.S, Geim A.K, Morozov S.V, Jiang D, Zhang Y, Dubonos S.V, et al. Electric field effect in atomically thin carbon films, Science. 2004; 306(5696): 666–669.

[20] Lee C, Wei X, Kysar J.W, Hone J, Measurement of

the elastic properties and intrinsic strength of monolayer graphene, Science. 2008; 321(5887): 385–388.
[21] Liu L, Zhou M, Jin L, Li L, Mo Y, Su G, et al. Recent advances in friction and lubrication of graphene and other 2D materials: Mechanisms and applications, Adv Colloid Interface Sci. 2019; 7: 199–216.
[22] Manafi D, Akbari D, Optimization of the Spot Weld Locations for Increasing the Joint Strength of the Welded Plates, Amirkabir J Mech Eng. 2019; 51(5): 1097–1105.
[23] Vural M, Akkus A, On the resistance spot weldability of galvanized interstitial free steel sheets with austenitic stainless steel sheets, J Mater Process Technol. 2004; 153: 1–6.
[24] Khosravi M, Mansouri M, Gholami A, Yaghoubinezhad Y, Effect of graphene oxide and reduced graphene oxide nanosheets on the microstructure and mechanical properties of mild steel jointing by flux-cored arc welding, Int J Miner Metall Mater. 2020; 27: 505–514.
[25] Wang S, Wei X, Xu J, Hong J, Song X, Yu C, et al. Strengthening and toughening mechanisms in refilled friction stir spot welding of AA2014 aluminum alloy reinforced by graphene nanosheets, Mater Des. 2020; 186: 108212.
[26] Isa M.S.M, Muhamad M.R, Yusof F, Yusoff N, Brytan Z, Suga T, et al. Improved mechanical and electrical properties of copper-aluminum joints with highly aligned graphene reinforcement via friction stir spot welding, J Mater Res Technol. 2023; 24: 9203–9215.
[27] Hummers W.S Jr, Offerman R.E. Preparation of graphitic oxide, J Am Chem Soc. 1958; 80(6): 1339.
[28] Jia H, Xu J, Lu L, Yu Y, Zuo Y, Tian Q, et al. Three-dimensional Au nanoparticles/nano-poly (3,4-ethylene dioxythiophene)-graphene aerogel nanocomposite: A high-performance electrochemical immunosensing platform for prostate-specific antigen detection, Sens Actuator B Chem. 2018; 260: 990–997.
[29] Taheridoustabad I, Khosravi M, Yaghoubinezhad Y. Fabrication of GO/RGO/TiC/TiB_2 nanocomposite coating on Ti–6Al–4V alloy using electrical discharge coating and exploring its tribological properties, Tribol Int. 2021; 156: 106860.
[30] Cheng L, Liu C, Han D, Ma S, Guo W, Cai H, et al. Effect of graphene on corrosion resistance of waterborne inorganic zinc-rich coatings, J Alloys Compd. 2019; 774: 255–264.
[31] Zhang Y, Chen F, Zhang Y, Du C. Influence of graphene oxide additive on the tribological and electrochemical corrosion properties of a PEO coating prepared on AZ31 magnesium alloy, Tribol Int. 2020; 146: 106135.